NANO LETTERS

LETTER

pubs.acs.org/NanoLett

Strong Enhancement of Solar Cell Efficiency Due to Quantum Dots with Built-In Charge

Kimberly A. Sablon,[†] John W. Little,[†] Vladimir Mitin,[‡] Andrei Sergeev,*[,‡] Nizami Vagidov,[‡] and Kitt Reinhardt[¶]

[†]U.S. Army Research Laboratory, Adelphi, Maryland 20783, United States

[‡]University at Buffalo, Buffalo, New York 14260, United States

[¶]AFOSR/NE, 875 North Randolph Street, Suite 326, Arlington, Virginia 22203, United States

Supporting Information

ABSTRACT: We report a 50% increase in the power conversion efficiency of InAs/GaAs quantum dot solar cells due to n-doping of the interdot space. The n-doped device was compared with GaAs reference cell, undoped, and p-doped devices. We found that the quantum dots with built-in charge (Q-BIC) enhance electron intersubband quantum dot transitions, suppress fast electron capture processes, and preclude deterioration of the open circuit voltage in the n-doped structures. These factors lead to enhanced harvesting and efficient conversion of IR energy in the Q-BIC solar cells.

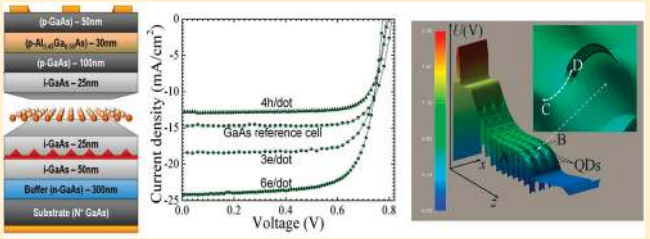

KEYWORDS: Solar cell, quantum dots, doping, infrared radiation, built-in charge

Quantum dot solar cells have been attractive for solar cell applications due to their ability to enhance light absorption via multiple energy levels introduced by quantum dots (QD) and extend the absorption edge into the infrared range.[1−5] Theoretical modeling of the intermediate band QD solar cell has predicted an increase in the efficiency up to ∼64% for a well-adjusted intermediate band,[5] but up to now the experimental works have shown very limited success.[6−10] In contrast to the expected substantial increase in the photocurrent due to harvesting of infrared energy, the enhanced recombination of photocarriers via dots does not allow for a noticeable improvement of the short circuit current, J_{SC}. Moreover, in many cases even a small increase of J_{SC} was accompanied by the deterioration of the open circuit voltage, V_{OC}.

The analogous concept of the impurity photovoltaic effect has been studied for many years. In the early sixties, Wolf proposed to use impurity levels to collect the long-wavelength radiation.[10] In response, Shockley and Queisser[11] argued that additional impurity levels drastically enhance the recombination processes (Shockley−Read−Hall recombination) and consequently deteriorate the device performance. Trade-off between IR energy harvesting and recombination losses due to impurity electron levels is a long-term problem studied without noticeable success in a number of theoretical and experimental investigations. However, compared to the midgap impurities, quantum dots offer more flexibility for nanoengineering of electron processes via dot size, correlation of dot positions, and selective doping. Research of QD solar cell capabilities is seen still far from completion.

In this work, we investigate the effects of the quantum dots with built-in charge (Q-BIC) on the solar energy harvesting and recombination processes. Two straightforward ideas that support this research are related to the expected positive effects of doping on V_{OC} and IR harvesting. First, we anticipate that, as in conventional heterojunction devices, doping will avert the deterioration of the open circuit voltage.[12] Second, we also expect that additional carriers in QDs created by doping will enhance the IR absorption and the photocurrent as shown in Figure 1 for n-doping. Figure 1a presents the processes in a QD structure without doping. Figure 1b,c shows the doping-induced process associated with electrons in the ground state due to intentional doping of dots. Figure 1c demonstrates a two-step process, where two electrons are excited by IR radiation to the excited localized QD state. Consequently, strong electron−electron interaction in QDs[13,14] causes one of these electrons to transfer to some low-energy state (for example, to the ground state) while another electron transfers to the conducting state and leaves the dot. The n-doping enhances electron transitions in QDs shown in Figure 1b,c without substantially changing the hole kinetics. In the same way, the p-doping enhances the hole transitions in QDs. Comparing electron and hole transitions in QDs, one should take into account that the electron energy level spacing in QDs is significantly larger than the spacing for holes due to the large effective mass of holes. The electron transitions in QDs significantly exceed the thermal energy and cannot be induced by thermal phonons. To stimulate these transitions by IR radiation, the n-doping should be preferable.

Received: February 17, 2011
Revised: April 27, 2011
Published: May 05, 2011

ACS Publications © 2011 American Chemical Society

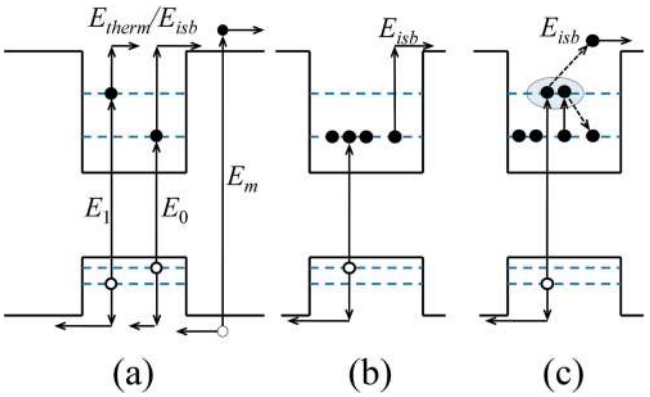

Figure 1. (a) Photogeneration of electron−hole pairs into the ground QD state (E_0) and into the excited QD state (E_1) followed by either thermionic emission (E_{therm}) or intersubband photoexcitation (E_{isb}) into the conducting channel; E_m is the direct photogeneration in the GaAs matrix. (b) Process induced by n-doping with IR transition of an electron from the localized to the conducting state. (c) Another doping-induced process, where the radiation excites two electrons to QD excited states, then due to strong interelectron interaction in a QD one of these electrons transfers to the conducting state and the other transfers to a low-energy state.

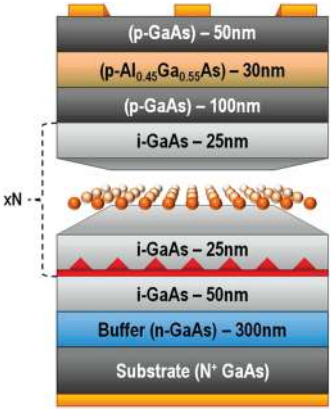

Figure 2. Growth diagram of a delta (δ)-doped QD structure.

A critical and challenging question that needs to be addressed is the effect of doping on the photocarrier capture rate and dot population. Like the quantum well population,[15] the dot population under a stationary light flux is determined by the condition of equal capturing for electrons and holes into a dot. Different electron and hole capture rates lead to an accumulation of the built-in charge and creation of potential barriers, which impede fast capture processes and accelerate slow processes. Thus, the dot population under light is determined by both doping and the carrier capture rates. There is a strong dependence of capture rates on the electric field even in relatively small fields.[16] Consequently, the built-in charge substantially affects the effective electric field around the dot thereby modifying capture processes. Thus, the harvesting of IR radiation (Figure 1b,c) and carrier capture are strongly interrelated via the built-in charge and corresponding barriers around dots.

To study effects of the built-in charge on the J_{SC}, V_{OC}, and efficiency, as well as to understand the IR-induced transitions and capture processes, we fabricated and investigated p- and n-doped InAs/GaAs QD solar cells with various doping levels. We measured the $I-V$ characteristics under light, spectral response, and photoluminescence. Finally, we present the data that shows the dependencies of solar cell parameters on doping. Our results show that n-doping of the interdot space improves solar energy conversion. For the most heavily doped sample, the photovoltaic efficiency improves by as much as 50% compared with an undoped device. Because we have not observed any evidence of the effect saturating, we can expect an even stronger enhancement of the photovoltaic efficiency for further increase of the doping level.

Figure 2 illustrates the growth diagram of a delta (δ)-doped QD structure in which a plane of dopants is placed in the middle of each GaAs layer that separates the dot layers. The structures were grown on n^+-GaAs (100) substrates by molecular beam epitaxy. Following oxide desorption, a 300 nm n^+-GaAs buffer with a doping density of 10^{18} cm^{-3} was grown at 595 °C. The substrate was cooled down to 530 °C for growth of the solar cell structure. QD growth occurred following the deposition of 2.1 MLs of InAs. The structures contain 20 stacks of QD layers separated by GaAs with dopant sheet densities of 0, 2.4×10^{10}, 3.6×10^{10}, 4.8×10^{10}, and 7.2×10^{10} cm^{-2} for providing zero, two, three, four, and six electrons per QD, respectively (based on average dot densities measured with transmission electron microscopy). The thickness of the GaAs spacer layer was 50 nm for all samples. The spacer thickness was chosen in an effort to dissipate strain fields in subsequent layers and hence reduce the strain accumulation and dislocations in the multistack samples. These relatively large spacers completely suppress electron tunneling between dots and prevent formation of the intermediate band. It will be shown that the localized levels in QDs provide efficient IR harvesting. The p^+-δ-n^+ structure (where δ refers to the δ-doped quantum dot layers) was completed by a 100 nm p-GaAs with a doping density of 1×10^{18} cm^{-3}, 30 nm p-$Al_{0.45}Ga_{0.55}As$ with a doping density of 5×10^{18} cm^{-3}, and finally a 50 nm p-GaAs contact layer with a doping density of 5×10^{18} cm^{-3}.

For characterization of the device performance, 250 μm circular solar cells were fabricated using standard photolithography followed by a phosphoric acid wet chemical etching. The structure was etched down into the n^+-GaAs substrate. Subsequently, an n-type blanket metallization of gold/tin/gold (15 nm/25 nm/250 nm thicknesses, respectively) was performed in an electron beam vacuum evaporator onto the back side of the substrate. Following blanket metallization, a rapid thermal annealing at 375 °C for 60 s was performed. Finally, the top of each mesa was patterned with a p-type metal ring contact. A chromium/gold contact layer (25 nm/250 nm thick, respectively) was deposited followed by a metal lift-off. The contact ring diameter is 200 μm with a 100 μm opening in the center to allow for top-side illumination. An array of these mesas was cleaved from the wafer and mounted in a 68 pin leaded chip carrier (LDCC) using indium metal. Wire bonds were attached to the top contact metal and out to a pin connection on the LDCC.

The $I-V$ characteristics of our devices were measured under light using a Newport Oriel PV calibrated solar simulator, which provides 1 Sun (AM1.5G) illumination. An Agilent 4156C precision semiconductor parameter analyzer was used to obtain the $I-V$ curves that are shown in Figure 3. Solar cell parameters such as the J_{SC}, V_{OC}, the fill factor FF, and the cell efficiency have been obtained from the resulting curves. While the p-doped device with the doping density of 4.8×10^{10} cm^{-2} shows

dx.doi.org/10.1021/nl200543v |Nano Lett. 2011, 11, 2311–2317

degradation in J_{SC} compared with the undoped device, the n-doped devices show a monotonic increase in J_{SC} with increasing of the doping level. Table 1 shows that, compared with the undoped device, the power conversion efficiency increases by 4.5, 30, and 50% for doping levels of 2, 3, and 6 electrons per dot, respectively.

In order to determine the harvesting role of IR photons in this radical improvement of the photovoltaic conversion efficiency, we measured the spectral dependence of the photocurrent under low illumination conditions using a Nicolet Fourier transform infrared (FTIR) spectrometer. Figure 4 shows the photoresponse of the GaAs reference cell, the undoped QD solar cell, and the QD solar cells doped to provide 2 electrons per dot. The band-to-band absorption in the GaAs matrix (E_m in Figure 1a) is observed below 880 nm. Transitions in the range from 880 to 920 nm correspond to the wetting layer.[17] Transitions above 920 nm are most likely related to the various excited QD states (e.g., E_1 in Figure 1a).[17] Finally, the ground state transition in QDs is 1100 nm (E_0 in Figure 1a). As seen, the photoresponse due to short-wavelength (above bandgap of GaAs) photons is reduced due to QDs, while the photoresponse contribution due to long-wavelength photons is enhanced. Doping further reduces the short-wavelength photoresponse related to the band-to-band transitions and transitions in the wetting layer but substantially enhances the IR photoresponse via QDs. The spectral density of the photocurrent monotonically decreases when the radiation wavelength increases up to 4.8 μm. As seen from the inset to Figure 4b for the sample with six electrons per dot, the spectral density shows a sharp rise at 4.8 μm (250 meV), which is believed to correspond to the transition from the dot ground state to the low energy resonance conducting state (E_{isb} in Figure 1b). In addition, a broad weak peak is observed between 4.8 and ~8 μm, which is close to the cutoff of the experiment. This peak decreases with doping decrease and is completely absent in the reference cell. Note that the analogous spectral dependencies and dependencies on doping have been observed in absorption of QD structures.[18]

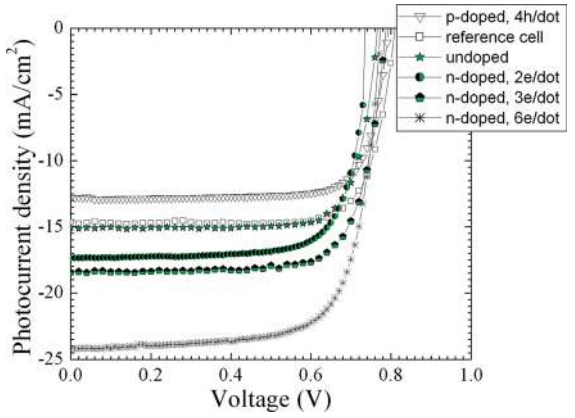

Figure 3. $I-V$ characteristics under 1 Sun (AM1.5 G) at 100 mW/cm^2 of QD solar cells as a function of doping: p-doped QD cell with 4 holes per dot, GaAs reference cell, undoped QD cell, n-doped QD cells with 2, 3, and 6 electrons per dot.

Table 1. QD Solar Cell Parameters

dot population	J_{SC} (mA/cm^2)	V_{OC} (V)	fill factor (%)	efficiency (%)
0	15.1	0.77	77	9.31
2	17.3	0.74	76	9.73
3	18.5	0.79	75	12.1
6	24.3	0.78	72	14.0

To investigate the cumulative contribution of the entire IR portion of the solar spectrum to the photoresponse of our devices, we measured the photocurrent under 1 Sun radiation using a GaAs filter, which eliminates photons with wavelengths less than 880 nm. The $I-V$ characteristics obtained with this filter, which were corrected for reflectivity losses, are presented in Figure 5. As expected, the GaAs reference cell does not show any photoresponse to the long-wavelength part of solar spectrum. The photoresponse due to radiation at wavelengths greater than 880 nm significantly increases with doping. In the device doped to provide two electrons per dot, we observe an increase in the photocurrent of 7.0 mA/cm^2 compared with the reference cell. The photocurrent from the sample with 6 electrons per dot increased by 9 mA/cm^2.

To study the effect of high energy photons on IR harvesting, we also investigated the IR photoresponse of QD structures under short-wavelength radiation. The InAs/AlGaAs QD structures were doped with Si in the middle of AlGaAs layers with a doping sheet concentration of 2.7×10^{11} cm^{-2}. A red LED with 620 nm wavelength was used for optical pumping. Figure 6 shows the photocurrent induced by 4300 nm IR radiation that corresponds to intersubband transitions in QDs. The measurements at 78 K demonstrate the increase of photocurrent by orders of magnitude due to the short-wavelength pumping. This observation manifests the strong enhancement of the IR electron transitions from the localized states in QDs to the conducting states in the matrix. Let us note that the QD structures used in

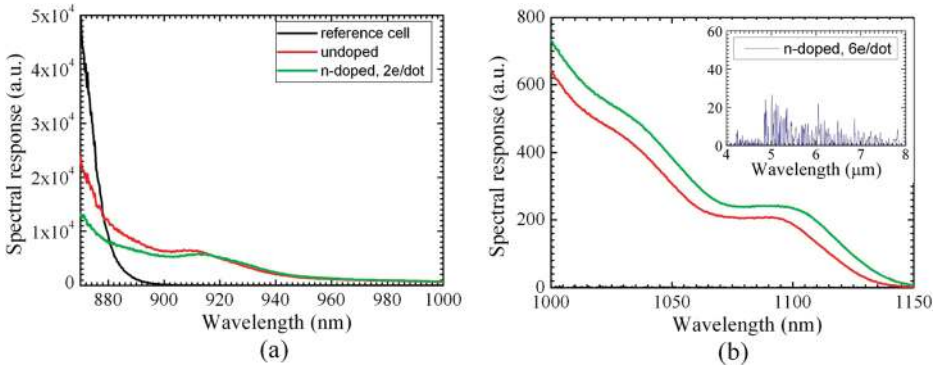

Figure 4. (a) Spectral response of the GaAs reference and doped and undoped QD structures. (b) Magnified view of the spectral response in the range from 1000 to 1150 nm. The inset shows the spectral response of QD structure with 6 e/dot in the range 4−8 μm.

dx.doi.org/10.1021/nl200543v |Nano Lett. 2011, 11, 2311–2317

these measurements were designed for IR photodetectors with large (up to 100) photoconductive gain, g, which strongly increases the photoresponse. Effect of optical pumping on IR harvesting in solar cells ($g = 1$) deserves special investigation.

To investigate mechanisms of carrier capture and evaluate effects of doping on the recombination losses, we studied the room temperature photoluminescence (PL) in our solar cells under short circuit conditions to match the conditions of previous $I-V$ measurements. The 532 nm line from a frequency-doubled neodymium doped yttrium aluminum garnet (Nd:YAG) laser was used to stimulate PL transitions. The diameter of the laser spot on a sample was 20 μm. The PL signal from the sample was dispersed by a monochromator and detected by an InGaAs detector array. The PL spectra were taken at 0.3 W/cm^2 excitation intensities. Figure 7a shows the dependence of the PL on the doping level in n-doped samples (the data for higher intensities are presented in the online Supporting Information). The PL intensity substantially increases with doping. This observation is associated with enhancing of intradot relaxation processes via electron−electron and hole−electron scattering in QDs due to electrons trapped in the dots.[19]

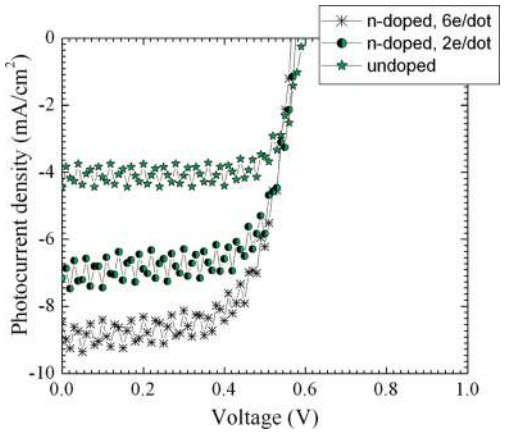

Figure 5. The long-wavelength photoresponse for undoped QD solar cell and n-doped cells with 2 and 6 electrons per dot under 1 Sun (AM1.5 G) light passed through short-wavelength GaAs absorber.

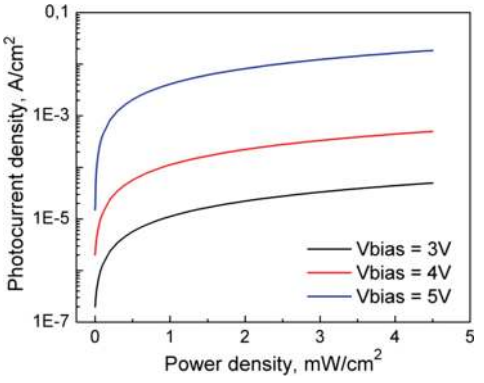

Figure 6. Photoresponse to the 4300 nm IR radiation of the QD structure under the 620 nm optical pumping.

Figure 7b shows the PL of p- and n-doped samples with the same level of doping, which corresponds to four carriers per dot. As seen, the PL intensity from the p-doped sample exceeds that of the n-doped sample by approximately 8 times. Thus, the p-doping substantially enhances capture and relaxation processes and increases the recombination losses. This observation is in agreement with experimental works in the area of QD lasers and light-emitting diodes, where it is well established that the p-doping strongly decreases the photocarrier lifetime and improves the efficiency of light-emitting diodes and modulation speed of QD lasers. Contrary to these devices, the QD solar cells require a long photocarrier lifetime. Therefore, n-doping proves to be more desirable for QD solar cells. In addition, the PL maximum of the p-doped sample is shifted toward the shorter wavelength regime with respect to the corresponding maximum for the n-doped sample. The observed energy shift of ~10 meV indicates substantial accumulation of holes in the p-doped QD structures.[20]

The most pronounced result of this work is the radical improvement of the photovoltaic efficiency due to enhanced harvesting of the IR portion of solar spectrum in n-doped QD solar cells. As shown in Figure 3, the photocurrent, J_{SC}, increases from 15.07 to 24.30 mA/cm^2 with increasing dot population. We also found that J_{SC} in the undoped QD solar cell is almost the same as that in the GaAs reference cell. The J_{SC} monotonically increases with increasing n-doping, but decreases due to p-doping. The scope of the data shows that the improvement of QD solar cell due to built-in charge should be associated with the doping-induced electron intersubband transitions, as presented in Figure 1b,c. To effectively contribute to the photovoltaic conversion, an electron and a hole should simultaneously escape from the dot. The energy level spacing for electrons in QDs is relatively large. It substantially exceeds the spacing for holes and the thermal energy. For this reason, it is precisely the electron

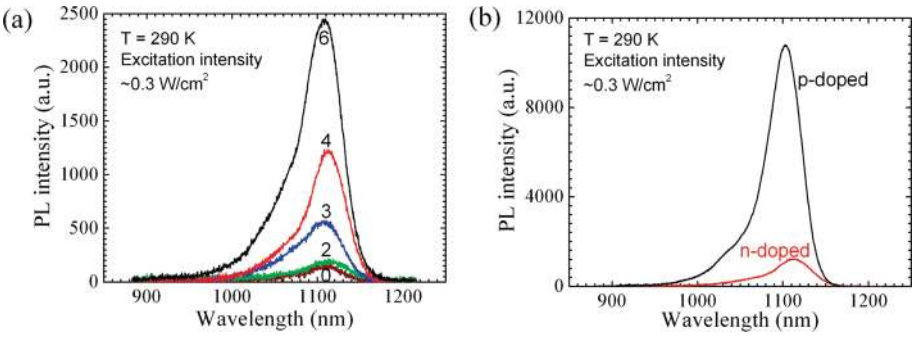

Figure 7. Room-temperature PL measurements at low excitation density for doped and undoped QD solar cells. (a) Dependence of the PL on the doping level for undoped device and n-doped devices with 2, 3, 4, and 6 electrons per dot and (b) comparison of PL in p- and n-doped devices with the same level of doping (4 carriers per dot).

dx.doi.org/10.1021/nl200543v |*Nano Lett.* 2011, 11, 2311–2317

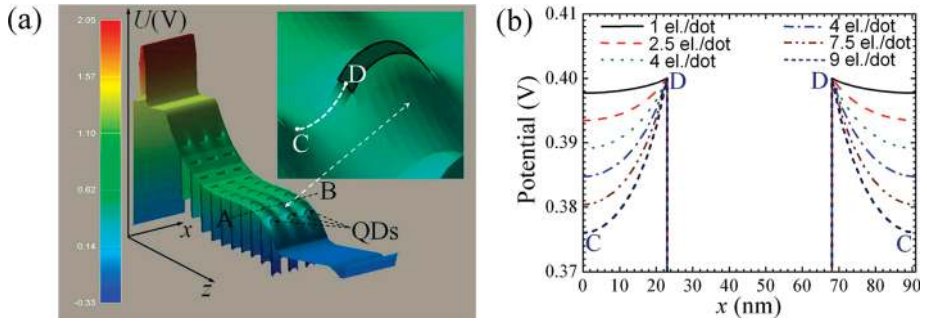

Figure 8. (a) The 3D potential profile of the conduction band in the QD solar cell with correlated positions of QDs. (Inset) Potential barriers around QD suppress the capture of photoelectrons. In the QD plane $A-B$, the potential between QDs varies from the maximum (D) to minimum (C). (b) Corresponding potential barriers for electrons in QD plane $A-B$ as a function of built-in electron charge.

intradot processes that limit the electron−hole escape from QDs. Thus, it is critically important to enhance the photoexcitation of electrons rather than holes.

Spectral response measurements in Figure 4 show partial contributions of the band-to-band, wetting layer, QD ground state, and QD subband transitions to the photocurrent. In agreement with the above interpretation, n-doping reduces the photocurrent generated by the band-to-band transitions and transitions in the wetting layer but substantially increases the IR harvesting via electron transitions shown in Figure 1b,c. The measurements of the photoresponse to IR portion of solar radiation (Figure 5) and its comparison with the photoresponse to the entire solar spectrum (Figure 3) demonstrate that even under a low-power radiation the short- and long-wavelength contributions are not independent and the total photocurrent is significantly larger than the sum of two separate contributions. Let us note that this effect is known for IR QD photodetectors, where the IR response is significantly enhanced by the optical pumping.[21] In ref 21, optical pumping was limited by relatively low energy quanta, which could generate only electron−hole pairs localized in the QDs. It was concluded that in this case the optical pumping is equivalent to the doping of QDs. The optical pumping with the energy quanta much larger than the GaAs bandgap also enhances by orders of magnitude the IR photoresponse (see Figure 6). The high-energy radiation increases the number of carriers captured into QDs, which in turn significantly enhances the IR electron transitions from localized states in QDs to the conducting states in matrix as it is shown in Figure 1b,c. As we discussed above, the same effect provides a significant increase in the photocurrent of Q-BIC solar cells.

Besides the effect of doping on the generation of mobile electron−hole pairs, doping affects the carrier capture and relaxation processes via the quantum dots with built-in charge. The photocarrier capture into QDs is usually associated with the inelastic processes accompanied by the emission of optical phonons. Despite many potential applications of QD structures in optoelectronics, there is still very limited and controversial information about capture rates for electrons and holes.[16,19,22] While in bulk materials the hole relaxation via emission of an optical phonon is faster than the corresponding electron relaxation, the relation between the capture rates in QDs appear to be the exact opposite. Experimental works, where both capture processes have been studied, show in favor of fast electron capture rate.[23−25] In ref 23, the ratio of hole and electron capture times, τ_c^p/τ_c^n, was determined to be 2 ps/0.5 ps = 4, whereas in ref 24 the same ratio was found to be an order of magnitude larger. As discussed for quantum-well structures by Ridley,[15] a difference in electron and hole capture rates should lead to an accumulation of a charge in the wells and to a formation of potential barriers around wells. The same effect is expected to be even more pronounced in QD structures.

To study potential barriers around QDs as a function of dot population, we used a simulation tool based on the nextnano[3] software,[26] which solves self-consistently Schrödinger and Poisson equations. Figure 8a shows the potential profile in QD structures with the position of dots correlated in QD planes. As seen, the potential barriers in the QD planes are smaller than those between QD planes. Therefore, the photoelectron capture via thermoexcitation is mainly expected to come from the QD planes. Figure 8b shows the potential barriers around single dots in QD planes as a function of the quantum dot population. According to these results, the barrier height is proportional to the number of electrons trapped in a dot, that is, $V_b = k_e n$, where n is the dot population and k_e = 2.5 meV. The coefficient k_e depends on the dot form and increases for smaller dots. The built-in negative charge suppresses the fast electron capture processes and accelerates the capture of holes. Taking into account an exponential dependence of the capture rates on the built-in charge,[27] the corresponding dot population may be evaluated as $n_d = (k_B T)/(2k_e)\ln(\tau_c^p/\tau_c^n)$ (see the online Supporting Information) . Therefore, even a relatively small difference in initial capture rates may provide a significant built-in charge. For example, for $\tau_c^p/\tau_c^n = 4$ obtained in ref 23 we get seven electrons localized in the dot. If the built-in charge is not provided by doping, the corresponding charge comes from p^+- and n^+-contacts and changes the potential profile in the active area. To avoid this negative effect, one should choose the doping level that provides the dot population n_d, which equates the electron and hole capture rates. Our estimate of the dot population based on the capture rates from ref 23 is obviously open to refinement, which will be done in future studies of Q-BIC solar cells with higher n-doping level.

Our investigations show that effects of doping on processes in Q-BIC solar cells are complex and interrelated. The undoped device demonstrates small, 0.5 mA/cm^2 increase in J_{SC} with respect to the GaAs reference cell (Figure 3), while the IR radiation itself gives an increase in the photocurrent of ~4 mA/cm^2 (Figure 5). These data show that in the undoped structures the significant positive effect of IR harvesting by QDs is eliminated by the recombination processes generated by QDs. Note that such small improvements in J_{SC} were observed in a number of previous works.[6−9] The situation radically changes with doping.

dx.doi.org/10.1021/nl200543v |Nano Lett. 2011, 11, 2311–2317

While the recombination processes are enhanced with doping (Figure 7), the doping-induced IR harvesting prevails over the recombination losses. The net positive effect increases with the doping level. At the doping level of two electrons per dot, J_{SC} increases by ~2.5 mA/cm^2 (Figure 3) and the IR radiation itself gives an increase in the photocurrent of ~7 mA/cm^2 (Figure 5). This shows that the recombination losses related to the conversion of short-wavelength radiation decrease the photocurrent by 4.5 mA/cm^2. At the doping level of six electrons per dot, J_{SC} increases by ~9 mA/cm^2 (Figure 3) and the IR radiation itself also gives an increase in the photocurrent of ~9 mA/cm^2 (Figure 5). However, this coincidence cannot be interpreted as additivity of partial spectral contributions to the photocurrent. At this doping level, the recombination losses related to the conversion of short-wavelength photons turn out to be compensated by the effect of optical pumping in the IR harvesting. As seen from the above discussion, these two effects are significant and require further investigations, in particular, at higher doping levels and higher intensities of radiation. One of the limitations on the doping level may originate due to the Auger recombination, which at the current doping levels remains substantially weaker than the Shockley−Read−Hall recombination.

It should be highlighted that in our devices, the strong enhancement of the photocurrent occurs without deterioration of the V_{OC}. This important improvement is exclusively due to the built-in charge. In previous works on structures without doping, even a small increase in J_{SC} was usually accompanied by a decrease in V_{OC}.[1−4,7−9] The positive influence of the doping on V_{OC} is not a specific feature of solely QD solar cells. It is understood for conventional pn-junction solar cells, that the minimum doping level is determined by the requirements of complete energy conversion.[12] In this case, the difference between the Fermi energies of electrons and holes in the active region under radiation should be smaller than the corresponding difference at the contacts. This in turn requires the concentration of majority carriers in the junction area to be at least as large as the concentration generated by illumination.[12] In practice,[28] this condition leads to a doping level of ~10^{16} cm^{-3}, which approximately corresponds to the doping in our structures.

We have established that the quantum dots with built-in charge enhance harvesting of IR energy. As it is summarized in Table 1, in Q-BIC solar cells the efficiency of the photovoltaic conversion increases from 9.3% in devices without doping to 14% in devices with the doping to provide six electrons per dot, which was the maximal doping level in our investigations. The photovoltaic efficiency as a function of the bias voltage is discussed in the online Supporting Information. We would like to note that the positive effect of Q-BIC is still far from saturation, that is, further improvements are expected with higher doping levels. The improvement of IR harvesting is anticipated to be even stronger at higher radiation intensities due to optical pumping effect. This makes the Q-BIC solar cells promising candidates for use with concentrators of solar radiation.

■ ASSOCIATED CONTENT

Supporting Information. (i) PL data for p- and n-doped QD structures at various excitation intensities; (ii) analytical description of the capture processes in QD structures; and (iii) discussion of the photovoltaic efficiency as a function of the bias voltage. This material is available free of charge via the Internet at http://pubs.acs.org.

■ AUTHOR INFORMATION

Corresponding Author
*E-mail: asergeev@buffalo.edu.

■ ACKNOWLEDGMENT

The authors thank Kimberley Olver for sample processing, Salamo's group at University of Arkansas for assisting with PL measurements, Fred Towner of Maxion Technologies, Inc. for MBE growth, and Peter Vogl and Stefan Birner from the Walter Schottky Institute, Technische Universitat Munchen for providing us with nextnano^3 software. This work was partially supported by ARL Extreme Energy Grant from the Power and Energy Division. The work of A.S. was also partially supported by DMR of NSF.

■ REFERENCES

(1) Nozik, A. J. *Nano Lett.* **2010**, *10*, 2735.
(2) Laghumavarapu, R. P.; El-Emawy, M.; Nuntawong, N.; Moscho, A.; Lester, L. F.; Huffaker, D. L. *Appl. Phys. Lett.* **2007**, *91*, 243115.
(3) Hubbard, S. M.; Raffaelle, R.; Robinson, R.; Bailey, C.; Wilt, D.; Wolford, D.; Maurer, W.; Bailey, S. *Mater. Res. Soc. Symp. Proc.* **2007**, *1017*, 13.
(4) Sablon, K. A.; Little, J. W.; Olver, K. A.; Wang, Zh.M.; Dorogan, V. G.; Mazur, Yu.I.; Salamo, G. J.; Towner, F. J. *J. Appl. Phys.* **2010**, *108*, 074305.
(5) Luque, A.; Marti, A. *Phys. Rev. Lett.* **1997**, *78*, 5014.
(6) Guimard, D.; Morihara, R.; Bordel, D.; Tanabe, K.; Wakayama, Y.; Nishioka, M.; Arakawa, Y. *Appl. Phys. Lett.* **2010**, *96*, 203507.
(7) Zhou, D.; Vullum, P. E.; Sharma, G.; Thomassen, S. F.; Holmestad, R.; Reenaas, T. W.; Fimland, B. O. *Appl. Phys. Lett.* **2010**, *96*, 083108.
(8) Hubbard, S. M.; Cress, C. D.; Bailey, C. G.; Raffaelle, R. P.; Bailey, S. G.; Wilt, D. M. *Appl. Phys. Lett.* **2008**, *92*, 123512.
(9) Oshima, R.; Takata, A.; Okada, Y. *Appl. Phys. Lett.* **2008**, *93*, 083111.
(10) Wolf, M. *Proc. IRE* **1960**, *48*, 1246.
(11) Shockley, W.; Queisser, H. J. *J. Appl. Phys.* **1961**, *32*, 510.
(12) Würfel, P. *Physics of Solar Cells: From Basic Principles to Advanced Concepts*; Wiley-VCH: Weinheim, Germany, 2005.
(13) Schaller, R. D.; Klimov, V. I. *Phys. Rev. Lett.* **2004**, *92*, 186601.
(14) Ellingson, R. J.; Beard, M. C.; Johnson, J. C.; Yu, P.; Micic, O. I.; Nozik, A. J.; Shabaev, A.; Efros, A. L. *Nano Lett.* **2005**, *5*, 865.
(15) Ridley, B. K. *Phys. Rev. B* **1994**, *50*, 1717.
(16) Geller, M.; Marent, A.; Stock, E.; Bimberg, D.; Zubkov, V. I.; Shulgunova, I. S.; Solomonov, A. V. *Appl. Phys. Lett.* **2006**, *89*, 232105.
(17) Blokhin, S. A.; Sakharov, A. V.; Nadtochy, A. M.; Pauysov, A. S.; Maximov, M. V.; Ledentsov, N. N.; Kovsh, A. R.; Mikhrin, S. S.; Lantratov, V. M.; Mintairov, S. A.; *Semiconductors* **2009**, *43*, 514.
(18) Popescu, V.; Bester, G.; Hanna, M. C.; Norman, A. G.; Zunger, A. *Phys. Rev. B* **2008**, *78*, 205321.
(19) Gundogdu, K.; Hall, K. C.; Boggess, T. F.; Deppe, D. G.; Shchekin, O. B. *Appl. Phys. Lett.* **2004**, *85*, 4570.
(20) Regelman, D. V.; Dekel, E.; Gershoni, D.; Ehrenfreund, E.; Williamson, A. J.; Shumway, J.; Zunger, A.; Schoenfeld, W. V.; Petroff, P. M. *Phys. Rev. B* **2001**, *64*, 165301.
(21) Höglund, L.; Holtz, P. O.; Pettersson, H.; Asplund, C.; Wang, Q.; Malm, H.; Almqvist, S.; Petrini, E.; Andersson, J. Y. *Appl. Phys. Lett.* **2009**, *94*, 053503.
(22) Muller, T.; Schrey, F. F.; Strasser, G; Unterrainer, K. *Appl. Phys. Lett.* **2003**, *83*, 3572.
(23) Yarotski, D. A.; Averitt, R. D.; Negre, N; Crooker, S. A.; Taylor, A. J.; Donati, G. P.; Stintz, A.; Lester, L. F.; Malloy, K. J. *J. Opt. Soc. Am. B* **2002**, *19*, 1480.
(24) Luque, A; Marti, A; Lopez, N; Antolin, E; Canovas, E; Stanley, C; Farmer, C; Diaz, P. *J. Appl. Phys.* **2006**, *99*, 094503.

(25) Badolato, A.; Hennessy, K.; Atature, M.; Dreiser, J.; Hu, E.; Petroff, P. M.; Imamoglu, A. *Science* **2005**, *308*, 1158.
(26) http://www.nextnano.de/nextnano3/overview/overview.htm. Access date February 17, 2010.
(27) (a) Sergeev, A.; Mitin, V; Stroscio, M. *Physica B* **2002**, *316-317*, 369. (b) Mitin, V.; Antipov, A.; Sergeev, A.; Vagidov, N; Eason, D.; Strasser, G. *Nanoscale Res. Lett.* **2011**, *6*, 21.
(28) Fahrenbruch, A. L.; Bube, R. H. *Fundamentals of Solar Cells: Photovoltaic Solar Energy Conversion*; Academic Press: New York, 1983.